Ab initio study of magneto-ionic mechanisms in ferromagnet/oxide multilayers

Ab initio study of magneto-ionic mechanisms in ferromagnet/oxide multilayers

Adriano Di Pietro,[1,2,*] Rohit Pachat,[3] Lei Qiao,[4,5] Liza Herrera-Diez,[3] Johannes W. van der Jagt,[6,7] Silvia Picozzi,[5] Dafiné Ravelosona,[3,6] Wei Ren,[4] and Gianfranco Durin[1]

[1]*Istituto Nazionale di Ricerca Metrologica, Strada delle Cacce 91, 10135 Torino, Italy*

[2]*Politecnico di Torino, Corso Duca degli Abruzzi 24, 10129 Torino, Italy*

[3]*Centre de Nanosciences et de Nanotechnologies, CNRS, Université Paris-Saclay, 10 Boulevard Thomas Gobert, 91120 Palaiseau, France*

[4]*Physics Department, International Center of Quantum and Molecular Structures, Materials Genome Institute, State Key Laboratory of Advanced Special Steel, Shanghai Key Laboratory of High Temperature Superconductors, Shanghai University, Shanghai 200444, China*

[5]*Consiglio Nazionale delle Ricerche (CNR-SPIN), Unità di Ricerca presso Terzi c/o Università "G. D'Annunzio," 66100 Chieti, Italy*

[6]*Spin-Ion Technologies, 10 Boulevard Thomas Gobert, 91120 Palaiseau, France*

[7]*Université Paris-Saclay, 3 rue Juliot Curie, 91190 Gif-sur-Yvette, France*

(Received 8 February 2022; revised 6 March 2023; accepted 12 April 2023; published 11 May 2023)

The application of gate voltages in heavy metal/ferromagnet/oxide multilayer stacks has been identified as one possible candidate to manipulate their anisotropy at will. However, this method has proven to show a wide variety of behaviors in terms of reversibility, depending on the nature of the metal/oxide interface and its degree of oxidation. In order to shed light on the microscopic mechanism governing the complex magneto-ionic behavior in Ta/CoFeB/HfO_2, we perform *ab initio* simulations on various setups comprising Fe/O and Fe/HfO_2 interfaces with different oxygen atom interfacial geometries. After the determination of the more stable interfacial configurations, we calculate the magnetocrystalline anisotropy energy on the different unit cell configurations and formulate a possible mechanism that well describes the recent experimental observations in Ta/CoFeB/HfO_2.

DOI: 10.1103/PhysRevB.107.174413

I. INTRODUCTION

The ever-increasing demand for memory storage in the modern information technology (IT) industry has made the need for new energy efficient storage alternatives all the more important. Voltage control of magnetic anisotropy (VCMA) [1] has gained scientific interest as one of the prime candidates to develop ultralow-energy memory storage devices [2–5] and is usually studied in two different variants: The first one aims at modifying the magnetic properties of thin films by pure charge accumulation/depletion effects induced by voltage application [4,6–8]. The second variant makes use of voltage-induced ionic motion in heavy metal (HM)/ferromagnet (FM)/oxide (Ox) thin film multilayers to carefully tune the oxygen/ferromagnet chemical and electrostatic interaction, enabling the control of magnetic anisotropy [3,9,10]. The main advantage of ionic manipulation in comparison to pure charge accumulation/depletion techniques is the nonvolatility of the magnetization switching, while the trade-off is a more complex reversibility mechanism combining ion mobility and chemical composition at the FM/Ox interface.

The work of Fassatoui *et al.* [11] clearly shows how the application of gate voltages causes a reversible magnetization switching in Pt/Co/AlOx as well as in Pt/Co/TbOx. At the same time, applying a gate voltage in Pt/Co/MgOx has the effect of irreversibly pushing the anisotropy easy axis out of plane. This discrepancy has been attributed to the result of the different character of the ionic mobility of the oxides: TbOx and AlOx have the common property of being oxides with a predominantly oxygen-based ionic mobility [11,12], while MgOx is known to have Mg as the principal ionic carrier under the application of gate voltages [13]. CoFeB/oxide multilayer structures are of great technological interest as they have shown promise for the design of nonvolatile, high-density memory storage devices owing to their high tunneling magnetoresistance (TMR), low damping, and perpendicular magnetic anisotropy (PMA) [14–16]. A recent work from Pachat *et al.* [17] highlighted a more complex magneto-ionic behavior in Ta/CoFeB/HfO_2 multilayers. The application of a gate voltage to the as-grown material with in-plane anisotropy (IPA) initially causes a nonvolatile, irreversible spin-reorientation transition (SRT) to a perpendicular anisotropy state (PMA). Further application of the gate voltage causes the transition to a fully reversible regime. This two-step process is in contrast with the picture presented in Ref. [11] because ionic mobility in HfO_2 is attributed to oxygen [18]. To formulate a hypothesis on the mechanism governing these different reversibility behaviors in Ta/CoFeB/HfO_2, we perform *ab initio* simulations using density functional theory (DFT) to determine

*a.dipietro@inrim.it

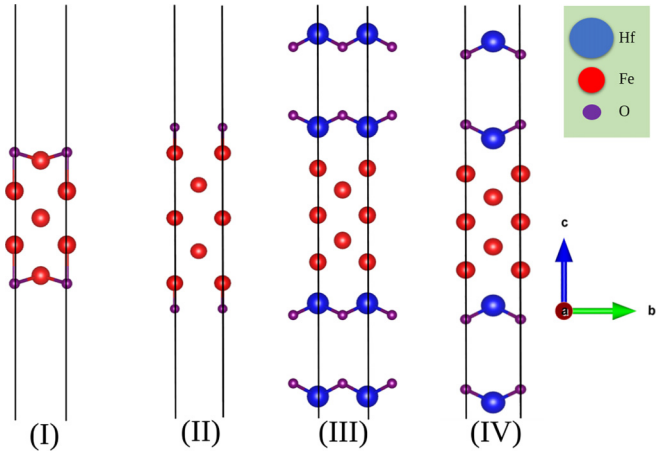

FIG. 1. Sketch of the different interfacial configurations. Unit cells (I) and (II) represent Fe/O interfaces while unit cells (III) and (IV) represent the Fe/HfO_2 interfaces.

the structural and magnetic properties of two FM/oxide interfaces.

The paper is structured as follows: In Sec. II, we provide the computational details of our simulations and a brief overview of the theoretical framework used to describe the magnetic anisotropy in FM/oxide interfaces. In Sec. III, we analyze the structural properties of two different FM/oxide interfaces, displaying either interstitial or frontal oxygen positioning [see Figs. 1 and 3(c)]. After having determined the optimal oxygen configurations of these setups, we compute the magnetic anisotropy energy of the Fe/HfO_2 unit cells. We also explore the role of ionic mobility in determining the magnetic anisotropy properties of Fe/HfO_2 interfaces and highlight how the energy costs involved in ionic mobility are different depending on the site occupied. In Sec. IV, we discuss the results and compare them to the experimental data [17] and theoretical predictions [7,19] in order to formulate a hypothesis for the appearance of different magneto-ionic regimes in $CoFeB/HfO_2$ multilayers. Finally, in Sec. V, we provide a summary of the findings and outline possible systems to analyze to further probe our hypothesis.

II. METHODS AND COMPUTATIONAL DETAILS

A. Structural relaxations

We perform structural relaxation using density functional theory and applying the full-potential linearized augmented plane-wave (FLAPW) method [20], as implemented in the FLEUR code [21]. In particular, we rely on the generalized gradient approximation for the exchange-correlation potential, as implemented by the Perdew-Burke-Ernzerhof (PBE) functional [22]. Since the simulation of amorphous systems

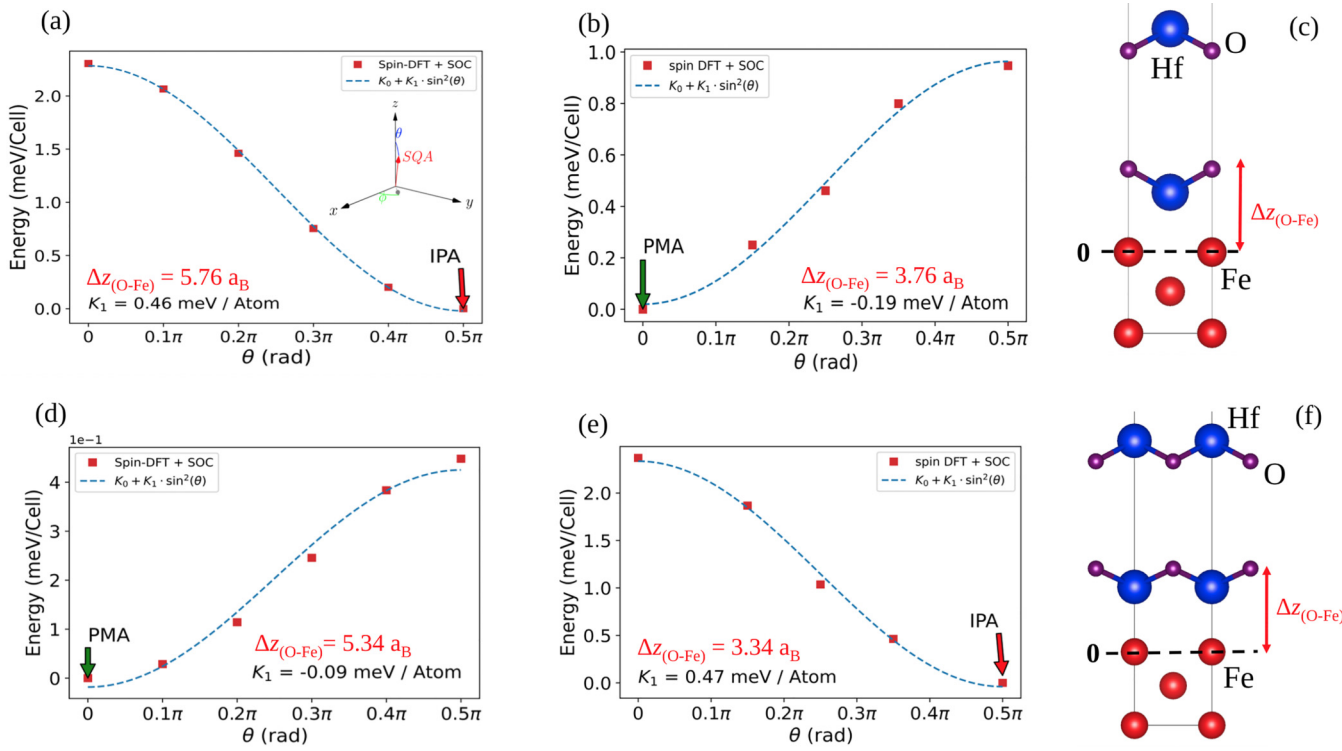

FIG. 2. Magnetocrystalline anisotropy energy (MCAE) comparison of the pure Fe/HfO_2 interface [structures (III) and (IV)]. The θ angle of the spin quantization axis (SQA) from Eq. (2) is shown in the inset of (a). (a), (b) MCAE for the ground state of the Fe/HfO_2 unit cell with a frontal O-Fe distance of (a) $\Delta z_{(O\text{-}Fe)} = 5.76 a_B$ (equilibrium) and (b) $\Delta z_{(O\text{-}Fe)} = 3.76 a_B$ (shifted). $\Delta z_{(O\text{-}Fe)}$ represents the interplanar distance of the interstitial oxygen species from the Fe surface (marked with the dashed line). (c) Fe/HfO_2 unit cell with frontal oxygen positioning. (d), (e) Ground state of the Fe/HfO_2 unit cell with interstitial interplanar O-Fe distance of (d) $\Delta z_{(O\text{-}Fe)} = 5.34 a_B$ (equilibrium) and (e) $\Delta z_{(O\text{-}Fe)} = 3.34 a_B$ (shifted). (f) Fe/HfO_2 unit cell with interstitial oxygen positioning. K_1 represents the value of the MCAE and is given by $E(\theta = 0) - E(\theta = \pi/2)$.

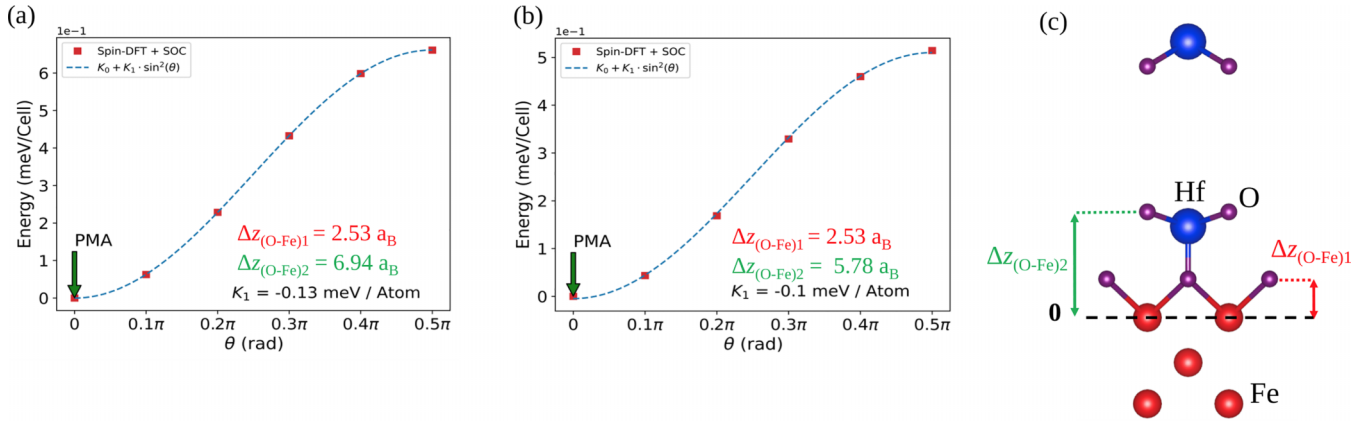

FIG. 3. Magnetocrystalline anisotropy energy (MCAE) [θ from Eq. (2)] in the Fe/HfO_2 setup shown with a shifted oxygen species at the interface. (a) MCAE of the mixed surface in its ground state. (b) MCAE of the mixed surface with a frontal O-Fe distance of 5.78a_B. (c) Side view of the Fe/HfO_2 unit cell with the mixed setup. $\Delta z_{(O\text{-}Fe)1}$ and $\Delta z_{(O\text{-}Fe)2}$ denote the interplanar distance of the frontal and interstitial oxygen species from the Fe surface, respectively (marked with the dashed line).

such as CoFeB is extremely challenging for *ab initio* methods, we reduced the ferromagnetic component of the system to the Fe atoms only. This approximation is justified on the basis of the composition of the $Co_{20}Fe_{60}B_{20}/HfO_2$ stacks studied in the literature, which are iron rich [17]. Furthermore, this approximation for CoFeB in *ab initio* simulations is commonly used in the literature [23]. We designed five different unit cells comprising an Fe/O interface [structures (I) and (II) in Fig. 1] composed of five magnetic layers (MLs) of Fe sandwiched between two monoatomic layers of oxygen on each side, an Fe/HfO_2 system [structures (III) and (IV) in Fig. 1] composed of 5 MLs of Fe atoms sandwiched between 2 MLs of HfO_2 on each side. Finally, to account for oxygen coming from the atmospheric interaction with the sample, we designed an Fe/HfO_2 system displaying both frontal and interstitial oxygen atoms [24]. This system is composed of 5 MLs of Fe atoms sandwiched between 2 MLs of HfO_2 on each side with an additional O layer located in the interstitial site of two Fe atoms [Fig. 3(c)]. We refer to this kind of system as "mixed interface" throughout this paper. The in-plane lattice constant of the system is fixed to the value of body-centered-cubic (bcc) Fe, i.e., $a_{Fe} = 2.87$ Å. To perform structural relaxation, we selected a cutoff value for the plane-wave basis of $K_{max} = 4.5a_B^{-1}$. We select the following values for the muffin-tin sphere radius of the atoms, $R_{MT}(Fe) = 2.18a_B$, $R_{MT}(Hf) = 2.54a_B$, $R_{MT}(O) = 1.19a_B$, and a k-point mesh of dimensions $10 \times 10 \times 1$. These parameters allow us to obtain self-consistent energies converged to at least 0.009 eV/atom. To determine the optimal interfacial configurations of oxygen atoms, structural relaxation is performed until the forces are smaller than 0.01 eV/Å.

B. Magnetocrystalline anisotropy energy (MCAE)

The *ab initio* calculation of the MCAE [25] is performed according to the following procedure [6,24,26]: After having determined the more stable interfacial geometries via the structural relaxation as outlined in Sec. II A, spin-orbit coupling (SOC) is treated in the second variation [27] in the Kohn-Sham Hamiltonian and the MCAE is computed by comparing the sums of one-electron energies via the magnetic force theorem [28,29]. This method is widely used and has been validated for transition metal interfaces [30]. The measurement of magnetocrystalline anisotropy requires an increased precision compared to structural relaxation: We therefore increase the size of the k-point mesh to $22 \times 22 \times 1$. Both with and without spin-orbit coupling, the plane-wave cutoff is kept at $K_{max} = 4.5a_B^{-1}$. With these parameters, we are able to obtain self-consistent energies converged to at least 0.01 meV/atom.[1] We remark how this contribution to the total magnetic anisotropy of the system is solely due to SOC and therefore neglects the contributions coming from dipole-dipole interactions (i.e., shape anisotropy effects). We neglect these terms in our discussion as the SOC in the presented system is lower than what can be found in actual multilayers (we do not add a heavy metal layer at the bottom of our unit cell) and their inclusion could unnecessarily hide the effects of oxygen on the anisotropy of the system.

C. Theoretical background

The origins of oxygen-enabled anisotropy manipulation in FM/oxide interfaces have been discussed extensively in the literature [19,24]. The underlying theoretical frameworks have been developed by Bruno [33] and van der Laan [34], which successfully linked a finite anisotropy in the orbital magnetic moment to an anisotropy contribution in the total energy in the presence of spin-orbit coupling. These theoretical frameworks predict a heavy dependence of the anisotropy energy on the exact shape and hybridization of the 3d orbitals. In this framework, oxygen atoms, when posed at a specific

[1]Some of the presented results, especially concerning equilibrium geometries, were benchmarked with the Vienna *ab initio* simulation package (VASP) [31,32]. The used simulation parameters were an energy cutoff of 500 eV and a k_{mesh} size $11 \times 11 \times 1$. The total energy convergence threshold was set to 10^{-6} eV and the structural relaxation convergence was set to a maximum force on each atom lower than 0.02 eV/Å.

distance, can have dramatic effects in the disruption of the otherwise almost isotropic magnetic moment distribution of the $3d$ orbitals of transition metal ferromagnets [24]. In particular, the $3d$ electrons of Fe tend to hybridize very effectively with the oxygen $2p_z$ orbitals. Therefore, depending on the relative position of Fe and O, the orbital character of the majority $3d$ orbitals will change. If, for instance, we imagine an oxygen atom sitting on top of an Fe atom, the atomic orbitals that are more likely to hybridize have an out-of-plane (OOP) character [35] $\{3d_{z^2}, 3d_{xz}, 3d_{yz}\}$. This results in a larger portion of occupied atomic orbitals with an in-plane character, i.e., $\{3d_{x^2-y^2}, 3d_{xy}\}$ orbitals. The orbital moment of the Fe atom will therefore point OOP and the anisotropy easy axis will follow it [24] according to the approximate analytic relation [33,34]

$$\Delta E_{\mathrm{SO}} = \xi_{\mathrm{SO}} \frac{\Delta\mu}{4\mu_B}, \tag{1}$$

where ΔE_{SO} represents the anisotropy energy, $\Delta\mu$ the orbital moment anisotropy, and ξ_{SO} the material-dependent spin-orbit coupling constant. We emphasize how this is an approximate relation that reproduces the results semiquantitatively but correctly reproduces the sign of the MCAE [36]. On the other hand, if the oxygen atom is located in the same plane as the Fe atom, hybridization is going to involve orbitals with in-plane (IP) character $\{3d_{x^2-y^2}, 3d_{xy}\}$. Fe atoms now retain a larger proportion of $3d$ orbitals with $\{3d_{z^2}, 3d_{xz}, 3d_{yz}\}$ orbital character which reverses the trend and shifts the orbital moment and the anisotropy easy axis in plane. Despite the thinness of the FM layers, one should always consider that the contributions to magnetic anisotropy are not limited to the first layer, but in fact often involve the second layer and possibly beyond [as in the case of Fe/MgO magnetic tunnel junctions (MTJs) [6]]. In addition, the appearance of magnetic anisotropy is still constrained by the symmetries of the crystal field that is coupled to the spin of the electrons via SOC. This implies that different lattice geometries have different angular dependencies of the anisotropy energy [33]. Layered systems with a cubic structure simple cubic (sc), fcc, or bcc and interfaces in the (001) direction (i.e., the ones we are concerned with) are predicted to have the uniaxial relation

$$\Delta E_{\mathrm{SO}} = K_0 + K_1 \sin^2\theta, \tag{2}$$

where θ is the spin quantization axis angle with respect to the $\hat{z}$ axis and K_0, K_1 represent material-dependent constants of anisotropy. An in-plane magnetic anisotropy (IPA) corresponds to the minimum of ΔE_{SO} for $\theta = \frac{\pi}{2}$, while perpendicular magnetic anisotropy (PMA) corresponds to the minimum of ΔE_{SO} for $\theta = 0$. This is the fitting function that we are going to use in all our MCAE calculations presented in Sec. III. We define our convention for MCAE as follows:

$$\mathrm{MCAE} = \Delta E_{\mathrm{SO}} = E(\theta = 0) - E(\theta = \pi/2). \tag{3}$$

III. RESULTS

A. Pure interfaces

As a first step, we perform structural relaxation on four different unit cells where we suppose that no interaction with atmospheric oxygen has taken effect (we refer to these as "pure interfaces"). Comparing Fig. 1 and Table I, we can observe how the optimal oxygen configurations change depending on the system considered: A pure Fe/O interface [structures (I) and (II) of Fig. 1] favors oxygen atoms to be located in the interstitial site with respect to Fe atoms. This preference appears to be reverted in the case of HfO_2, where a frontal, i.e., top positioning of oxygen atoms with

TABLE I. Total energy difference between the relaxed structures of Fig. 1.

$E_{(\mathrm{II})} - E_{(\mathrm{I})}$	$E_{(\mathrm{III})} - E_{(\mathrm{IV})}$
6.4 eV/cell	2.1 eV/cell

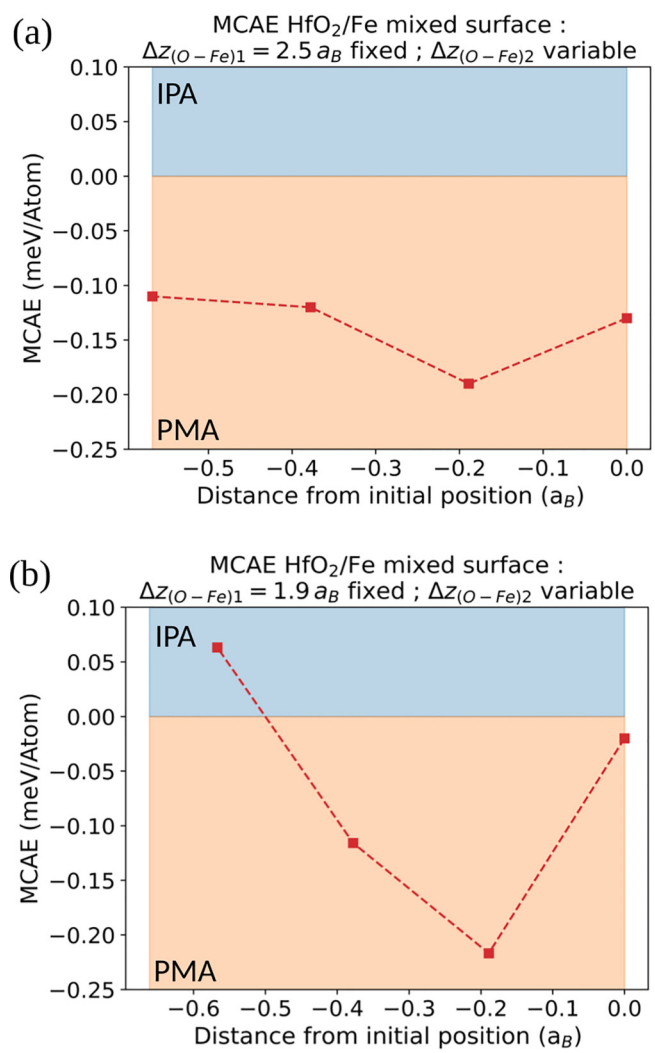

FIG. 4. Magnetocrystalline anisotropy energy (MCAE) as a function of the frontal and interstitial oxygen atom interplanar distances as depicted in Fig. 3(c). (a) Effect of frontal oxygen shifts ($\Delta z_{(\mathrm{O\text{-}Fe})2}$ variable) while the interstitial oxygen is kept fixed at a distance $\Delta z_{(\mathrm{O\text{-}Fe})2} = 2.53 a_B$ from the FM surface. (b) Effect of frontal oxygen shifts ($\Delta z_{(\mathrm{O\text{-}Fe})2}$ variable) while the interstitial oxygen is kept fixed at a distance $\Delta z_{(\mathrm{O\text{-}Fe})2} = 1.96 a_B$ from the FM surface. The initial interplanar distance of the frontal oxygen atoms is $\Delta z_{(\mathrm{O\text{-}Fe})2} = 6.94 a_B$ in both (a) and (b).

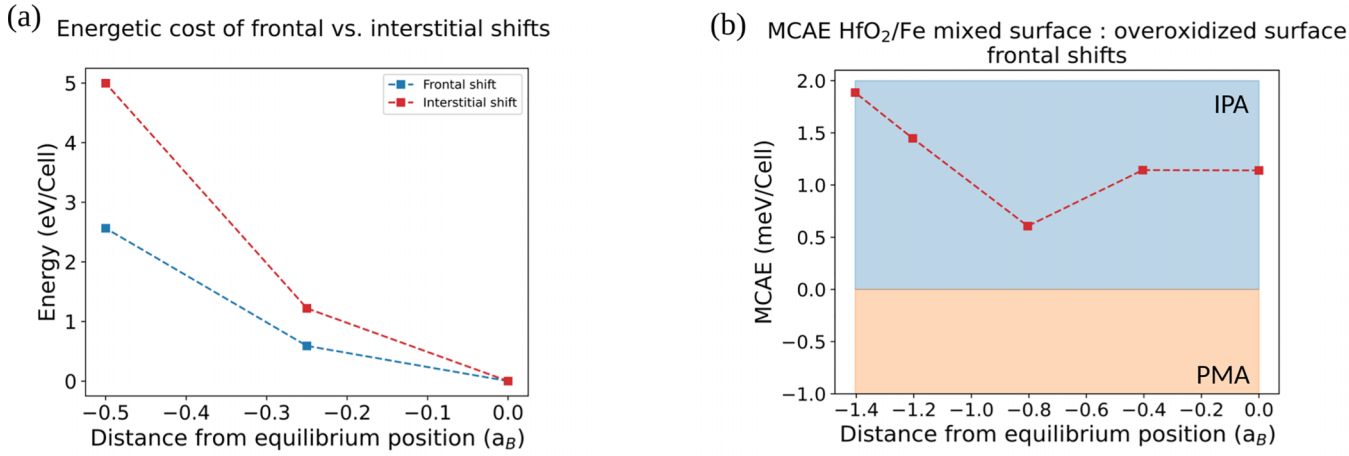

FIG. 5. (a) Energetic cost of shifting interstitial and frontal oxygen atoms in the mixed interface setup displayed in Fig. 3(c). The starting positions are $\Delta z_{(\text{O-Fe})1} = 2.53a_B$ for the interstitial oxygen atom and $\Delta z_{(\text{O-Fe})2} = 6.94a_B$ for the frontal oxygen atoms [i.e., the setup of Fig. 3(a)]. (b) MCAE at different frontal oxygen positions $\Delta z_{(\text{O-Fe})2}$ represented in Fig. 3(d). The starting positions are $\Delta z_{(\text{O-Fe})1} = -0.08a_B$ for the interstitial oxygen atom and $\Delta z_{(\text{O-Fe})2} = 6.94a_B$ for the frontal oxygen atoms [i.e., the setup of Fig. 3(c)]. Positive values on the y axis indicate that the system has IP magnetic anisotropy.

respect to the Fe atoms, seems to be strongly favored. After having determined the optimal configurations for the different unit cells, we include spin-orbit coupling to compute their magnetic anisotropy energy. In this case we focus specifically on the Fe/HfO_2 interface. By observing Fig. 2 we notice how the more stable frontally aligned oxygen setup [structure (IV) of Fig. 1] displays IP magnetic anisotropy [Fig. 2(a)], whereas an interstitial oxygen configuration [structure (III) of Fig. 1] yields PMA [Fig. 2(d)]. At this point, we introduce vertical ionic displacements (with respect to equilibrium configurations) on the interfacial oxygen atoms and recalculate the magnetic anisotropy. For simplicity, in all this analysis the Hf atoms are kept fixed. We notice that, by shifting the frontal oxygen atom in order to reduce the O-Fe distance by $\approx 2a_B$, we are able to achieve PMA [Fig. 2(b)]. As a side note, we remark how shifting the interstitial oxygen atom of structure (III) in Fig. 1 has the effect of recovering IP magnetic anisotropy [Fig. 2(e)].

B. Mixed Fe/HfO_2 interface

The application of a gate voltage is known to cause the oxidation of the FM surface. We model this effect by designing an Fe/HfO_2 unit cell displaying both interstitial and frontal oxygen alignment at the interface [see Fig. 3(c)]. By analyzing the effect on the magnetic anisotropy of different oxygen species mobility, we can get some hints on the microscopic mechanism governing magneto-ionic regimes in an experimental, more disordered scenario. As can be seen in Fig. 3(a), the relaxed structure with both frontal and interstitial oxygen displays OOP magnetic anisotropy. If we shift the frontal oxygens (while keeping the interstitial species still) by a nominal distance of $1.16a_B$, we notice little effect on magnetic anisotropy [Figs. 3(b) and 4(a)]. If, on the other hand, we shift the interstitial oxygen atom $1.96a_B$ from the FM surface, we notice how the MCAE becomes sensitive to frontal oxygen shifts and displays switching for a frontal shift of $0.74a_B$ [Fig. 4(b)]. Despite having checked the effect of oxygen shifts on anisotropy manipulation in this mixed surface setup, we expect the ionic mobility behavior of these two oxygen species to be different given their different environment. By observing Fig. 5(a), we can see that the energy cost of a frontal shift is lower than the energy cost of an interstitial shift, in accordance with our expectations. The energy costs are obtained by comparing the energy of identical unit cells that differ only by the position of the frontal/interstitial oxygen atom [37]. We point out how the disruption of PMA can also be obtained by only pushing the interstitial oxygens deeper in the ferromagnetic layer [Fig. 5(c)] [24]. From Fig. 5(c) we can however observe that once PMA is destroyed by this type of oxygen incorporation, it cannot be restored by moving the frontal oxygen atoms closer to the surface. This observation is also in agreement with the experiments [17], where samples that were exposed to a negative gate voltage for long times (for a reference of the field direction, see Fig. 6) did not display any reversibility of the voltage-induced SRT.

IV. DISCUSSION

Considering the results presented above, we propose the following hypothesis for the appearance of different magneto-ionic regimes in Ta/HfO_2/CoFeB. We once more highlight how we are assuming that the SRT caused by magneto-ionic effects in these systems is largely due to the MCAE changes (i.e., the part of magnetic anisotropy due to spin-orbit coupling [33]). We do not discuss the effects of shape anisotropy in the present study as oxygen migration effects are expected to cause the most significant changes to magnetic anisotropy via the hybridization and SOC effects described in Sec. II B [33]. As can be seen from Figs. 2(a) and 1, the pure Fe/HfO_2 surface with frontally aligned oxygens appears to be both the more stable structure and the one displaying IP magnetic anisotropy [Fig. 6(a)]. This is in accordance with the experimental observation, where samples in the as-grown

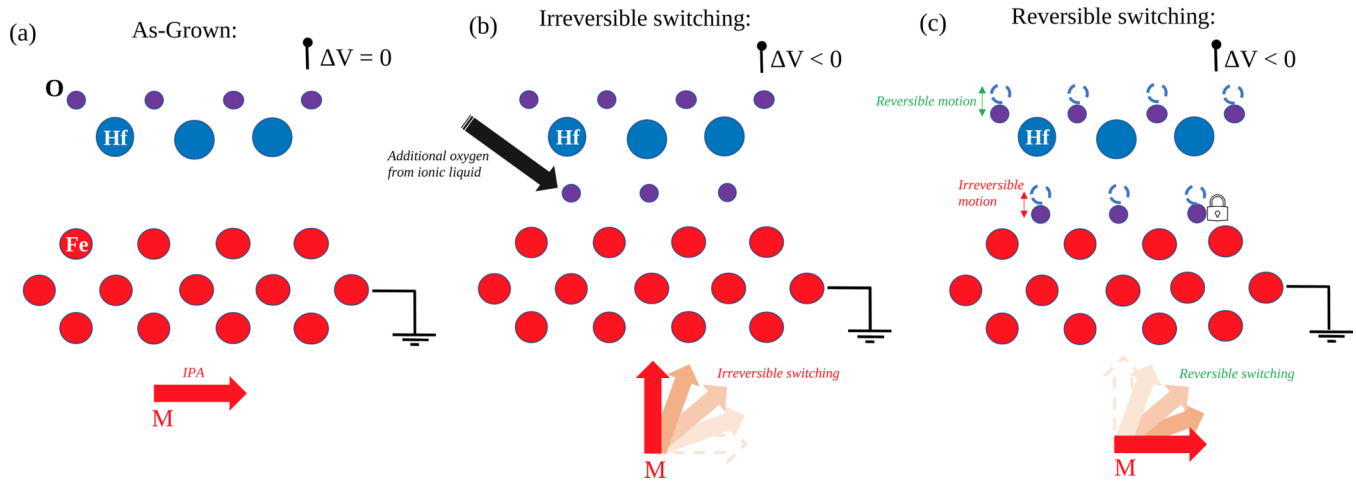

FIG. 6. Hypothesis for the mechanism governing the different magneto-ionic regimes in CoFeB/HfO_2 multilayers. (a) Ground state of the system. (b) Irreversible magnetization switching via interstitial sites occupied by migrating oxygen species. (c) Reversible magnetization switching via frontal oxygen shifts. The bottom cartoon in all three panels represents the magnetization direction and the switching process.

form displayed IP magnetic anisotropy [17]. As observed in Ref. [17], the application of a negative gate voltage across Ta/CoFeB/HfO_2 results in an irreversible SRT from IPA to PMA caused by the diffusion of oxygen species towards the CoFeB layer. We model this irreversible switching with the relaxed Fe/HfO_2 surface with both frontal and interstitial oxygens [Fig. 3(c)]. We hypothesize that in this first regime the frontal oxygen atoms are too far away to contribute to the anisotropy manipulation [Fig. 3(b)]. In contrast, the oxygens diffusing towards the surface and occupying the interstitial sites have a strong impact on the anisotropy of the system and induce PMA [Fig. 3(a)]. We therefore suggest that the initial irreversible anisotropy change in Ta/CoFeB/HfO_2 could be due to the irreversible occupation of the interstitial interface sites [Fig. 6(b)]. Once PMA is achieved, experimental observation [17] shows that the application of the gate voltage beyond the PMA state has the effect of pushing the magnetic anisotropy easy axis in plane, albeit in a reversible way. Our results suggest that this switch to a reversible behavior beyond PMA could be explained by the following: The continued application of the gate voltage has the effect of mobilizing frontal and interstitial oxygen species. As can be seen on Fig. 3(b), the MCAE is not sensitive to the frontal oxygen shifts at first. If, on the other hand, we shift the interstitial oxygen closer to the Fe surface by $0.57a_B$, we notice how the MCAE becomes sensitive to the shift of the frontal oxygen atoms and can be switched [Fig. 4(b)]. Furthermore, from Fig. 5(a), we know that mobilizing the interstitial oxygen atoms is more difficult than mobilizing the frontal ones: This could be to due the stronger bonding of the interstitial oxygen species with the superficial Fe atoms. This observation suggests that the reversibility of the anisotropy switching beyond the initial PMA could be largely attributed to frontal oxygen shifts [Fig. 6(c)]. As shown in Fig. 3(b), the transition PMA → IPA can also be achieved by shifting the interstitial oxygens deeper inside the ferromagnetic layer. We do not attribute the reversible manipulation of anisotropy beyond the initial PMA to these oxygen species because, once the anisotropy is shifted in plane by means of the interstitial oxygen species being pushed deeper in the sample, it is impossible to manipulate the magnetic anisotropy of the system by shifting the frontal oxygen species closer to the Fe surface [as displayed in Fig. 5(c)].

V. CONCLUSION

In this work we performed an *ab initio* analysis of the interplay between oxygen ionic mobility and anisotropy manipulation in two FM/oxide interfaces in order to formulate a hypothesis for the appearance of magneto-ionic regimes in Ta/CoFeB/HfO_2 stacks [17]. We found out that the different nature of the oxide at the interface plays an important role in determining the optimal interfacial oxygen geometry. In particular, we discovered how the pure Fe/HfO_2 interface displays a preferential frontal oxygen alignment which corresponds to an IP magnetic anisotropy. We observed how frontal oxygen mobility can induce PMA [4]. The inclusion of oxygen species in additional interstitial sites was investigated in order to determine their role in the appearance of magneto-ionic regimes [17]. We have shown how in these so-called mixed surfaces, the ionic mobility of frontal oxygen species is energetically more favorable than the mobility of interstitial ones. We have also shown how the interplay of mobility between these two different oxygen species can change the magnetic anisotropy of the sample. We conclude that the irreversibility of the transition between IPA (underoxidized) and PMA (optimally oxidized) could be mainly due to the interaction of the interstitial oxygen of the mixed surface and that the reversibility of the second regime is due to the mobility of the frontal oxygen species of the pure and mixed surface (Fig. 6). We point out how the Ta/CoFeB/HfO_2 multilayer in Ref. [17] is composed by amorphous materials that do not display the ordered structure of our unit cells. In spite of this difference, we find qualitative agreement between our results and the

ones reported in Ref. [17] and are therefore led to believe that anisotropy manipulation in these kinds of systems may be a consequence of relative FM/oxygen positioning localized at the interface. To further probe the validity of the hypothesis, one could analyze the relative range of magneto-ionic regimes in $Ta/CoFeB/HfO_2$ samples with different degrees of atmospheric oxygen interaction. We predict that the extreme case where there has been little to no exposure to atmospheric oxygen should result in a purely reversible system. In addition, a comparison between crystalline and polycrystalline structures could provide hints on the role played by the amorphous nature of the materials. Understanding in closer detail the interplay between ionic mobility and magnetic property tuning could prove very useful for the optimization of highly energy efficient read/write mechanisms for next-generation memory storage devices.

ACKNOWLEDGMENTS

This project has received funding from the European Union's Horizon 2020 research and innovation programme under the Marie Skłodowska-Curie Grant Agreement No. 860060 "Magnetism and the effect of Electric Field" (MagnEFi). Computational resources were provided by HPC@POLITO, a project of Academic Computing within the Department of Control and Computer Engineering at the Politecnico di Torino [38].

[1] R.-A. One, H. Béa, S. Mican, M. Joldos, P. B. Veiga, B. Dieny, L. D. Buda-Prejbeanu, and C. Tiusan, Route towards efficient magnetization reversal driven by voltage control of magnetic anisotropy, Sci. Rep. **11**, 8801 (2021).

[2] J. Suwardy, M. Goto, Y. Suzuki, and S. Miwa, Voltage-controlled magnetic anisotropy and Dzyaloshinskii-Moriya interactions in CoNi/MgO and CoNi/Pd/MgO, Jpn. J. Appl. Phys. **58**, 060917 (2019).

[3] B. Dieny and M. Chshiev, Perpendicular magnetic anisotropy at transition metal/oxide interfaces and applications, Rev. Mod. Phys. **89**, 025008 (2017).

[4] A. Hallal, H. X. Yang, B. Dieny, and M. Chshiev, Anatomy of perpendicular magnetic anisotropy in Fe/MgO magnetic tunnel junctions: First-principles insight, Phys. Rev. B **88**, 184423 (2013).

[5] A. Belabbes, G. Bihlmayer, S. Blügel, and A. Manchon, Oxygen-enabled control of Dzyaloshinskii-Moriya Interaction in ultra-thin magnetic films, Sci. Rep. **6**, 24634 (2016).

[6] F. Ibrahim, H. X. Yang, A. Hallal, B. Dieny, and M. Chshiev, Anatomy of electric field control of perpendicular magnetic anisotropy at Fe/MgO interfaces, Phys. Rev. B **93**, 014429 (2016).

[7] Z. Huang, I. Stolichnov, A. Bernand-Mantel, J. Borrel, S. Auffret, G. Gaudin, O. Boulle, S. Pizzini, L. Ranno, L. H. Diez, and N. Setter, Ferroelectric control of magnetic domains in ultra-thin cobalt layers, Appl. Phys. Lett. **103**, 222902 (2013).

[8] M. K. Niranjan, C. G. Duan, S. S. Jaswal, and E. Y. Tsymbal, Electric field effect on magnetization at the Fe/MgO(001) interface, Appl. Phys. Lett. **96**, 222504 (2010).

[9] S. Monso, B. Rodmacq, S. Auffret, G. Casali, F. Fettar, B. Gilles, B. Dieny, and P. Boyer, Crossover from in-plane to perpendicular anisotropy in Pt/CoFe/AlOx sandwiches as a function of Al oxidation: A very accurate control of the oxidation of tunnel barriers, Appl. Phys. Lett. **80**, 4157 (2002).

[10] U. Bauer, L. Yao, A. J. Tan, P. Agrawal, S. Emori, H. L. Tuller, S. van Dijken, and G. S. Beach, Magneto-ionic control of interfacial magnetism, Nat. Mater. **14**, 174 (2015).

[11] A. Fassatoui, J. P. Garcia, L. Ranno, J. Vogel, A. Bernand-Mantel, H. Béa, S. Pizzini, and S. Pizzini, Reversible and Irreversible Voltage Manipulation of Interfacial Magnetic Anisotropy in Pt/Co/Oxide Multilayers, Phys. Rev. Appl. **14**, 064041 (2020).

[12] H. G. Flynn, Transport phenomena, Phys. Today **15** (6), 96 (1962).

[13] N. Wu, W. Wang, Y. Wei, and T. Li, Studies on the effect of nano-sized MgO in magnesium-ion conducting gel polymer electrolyte for rechargeable magnesium batteries, Energies **10**, 1215 (2017).

[14] T. Liu, Y. Zhang, J. W. Cai, and H. Y. Pan, Thermally robust Mo/CoFeB/MgO trilayers with strong perpendicular magnetic anisotropy, Sci. Rep. **4**, 5895 (2014).

[15] S. Ikeda, K. Miura, H. Yamamoto, K. Mizunuma, H. D. Gan, M. Endo, S. Kanai, J. Hayakawa, F. Matsukura, and H. Ohno, A perpendicular-anisotropy CoFeB-MgO magnetic tunnel junction, Nat. Mater. **9**, 721 (2010).

[16] L. Z. Wang, X. Li, T. Sasaki, K. Wong, G. Q. Yu, S. Z. Peng, C. Zhao, T. Ohkubo, K. Hono, W. S. Zhao, and K. L. Wang, High voltage-controlled magnetic anisotropy and interface magnetoelectric effect in sputtered multilayers annealed at high temperatures, Sci. China: Phys. Mech. Astron. **63**, 277512 (2020).

[17] R. Pachat, D. Ourdani, J. W. van der Jagt, M.-A. Syskaki, A. D. Pietro, Y. Roussigné, S. Ono, M. S. Gabor, M. Chérif, G. Durin, J. Langer, M. Belmeguenai, D. Ravelosona, and L. H. Diez, Multiple Magnetoionic Regimes in $Ta/Co_{20}Fe_{60}B_{20}/HfO_2$, Phys. Rev. Appl. **15**, 064055 (2021).

[18] M. Schie, M. P. Müller, M. Salinga, R. Waser, and R. A. De Souza, Ion migration in crystalline and amorphous HfO_x, J. Chem. Phys. **146**, 094508 (2017).

[19] S. H. Liang, T. T. Zhang, P. Barate, J. Frougier, M. Vidal, P. Renucci, B. Xu, H. Jaffrès, J. M. George, X. Devaux, M. Hehn, X. Marie, S. Mangin, H. X. Yang, A. Hallal, M. Chshiev, T. Amand, H. F. Liu, D. P. Liu, X. F. Han *et al.*, Large and robust electrical spin injection into GaAs at zero magnetic field using an ultrathin CoFeB/MgO injector, Phys. Rev. B **90**, 085310 (2014).

[20] O. K. Andersen, Linear methods in band theory, Phys. Rev. B **12**, 3060 (1975).

[21] Fleur code: www.flapw.de.

[22] J. P. Perdew, M. Ernzerhof, and K. Burke, Rationale for mixing exact exchange with density functional approximations, J. Chem. Phys. **105**, 9982 (1996).

[23] W. Lin, B. Yang, A. P. Chen, X. Wu, R. Guo, S. Chen, L. Liu, Q. Xie, X. Shu, Y. Hui, G. M. Chow, Y. Feng,

G. Carlotti, S. Tacchi, H. Yang, and J. Chen, Perpendicular Magnetic Anisotropy and Dzyaloshinskii-Moriya Interaction at an Oxide/Ferromagnetic Metal Interface, Phys. Rev. Lett. **124**, 217202 (2020).

[24] H. X. Yang, M. Chshiev, B. Dieny, J. H. Lee, A. Manchon, and K. H. Shin, First-principles investigation of the very large perpendicular magnetic anisotropy at Fe|MgO and Co|MgO interfaces, Phys. Rev. B **84**, 054401 (2011).

[25] P. Strange, J. B. Staunton, B. L. Györffy, and H. Ebert, First principles theory of magnetocrystalline anisotropy, Phys. B: Condens. Matter **172**, 51 (1991).

[26] B. Zimmermann, G. Bihlmayer, M. Böttcher, M. Bouhassoune, S. Lounis, J. Sinova, S. Heinze, S. Blügel, and B. Dupé, Comparison of first-principles methods to extract magnetic parameters in ultrathin films: Co/Pt(111), Phys. Rev. B **99**, 214426 (2019).

[27] M. Heide, G. Bihlmayer, and S. Blügel, Describing Dzyaloshinskii-Moriya spirals from first principles, Phys. B: Condens. Matter **404**, 2678 (2009).

[28] M. Weinert, R. E. Watson, and J. W. Davenport, Total-energy differences and eigenvalue sums, Phys. Rev. B **32**, 2115 (1985).

[29] X. Wang, D. S. Wang, W. Ruqian, and A. J. Freeman, Validity of the force theorem for magnetocrystalline anisotropy, J. Magn. Magn. Mater. **159**, 337 (1996).

[30] P. Błoński and J. Hafner, Density-functional theory of the magnetic anisotropy of nanostructures: An assessment of different approximations, J. Phys.: Condens. Matter **21**, 426001 (2009).

[31] G. Kresse and J. Furthmüller, Efficiency of ab-initio total energy calculations for metals and semiconductors using a plane-wave basis set, Comput. Mater. Sci. **6**, 15 (1996).

[32] G. Kresse and J. Furthmüller, Efficient iterative schemes for *ab initio* total-energy calculations using a plane-wave basis set, Phys. Rev. B. **54**, 11169 (1996).

[33] P. Bruno, Tight-binding approach to the orbital magnetic moment and magnetocrystalline anisotropy of transition-metal monolayers, Phys. Rev. B **39**, 865 (1989).

[34] G. van der Laan, Microscopic origin of magnetocrystalline anisotropy in transition metal thin films, J. Phys.: Condens. Matter **10**, 3239 (1998).

[35] W. H. Butler, Tunneling magnetoresistance from a symmetry filtering effect, Sci. Technol. Adv. Mater. **9**, 014106 (2008).

[36] M. Košuth, V. Popescu, H. Ebert, and G. Bayreuther, Magnetic anisotropy of thin Fe films on GaAs, Europhys. Lett. **72**, 816 (2005).

[37] A. Kyritsakis, E. Baibuz, V. Jansson, and F. Djurabekova, Atomistic behavior of metal surfaces under high electric fields, Phys. Rev. B **99**, 205418 (2019).

[38] http://hpc.polito.it.